Journal of Veterinary Internal Medicine
Open Access

Case Report
J Vet Intern Med 2015;29:1638–1642

Coextensive Meningioma and Cholesterol Granuloma in the Forebrain of a Cat

P. Chawla, L. Cook, L. Himmell, L. Zekas, and M. Oglesbee

Key words: Feline; Magnetic resonance imaging; Pathology; Tumor.

A 9-year-old, female, spayed, domestic longhaired cat presented to The Ohio State University Veterinary Medical Center Oncology Service with a 6-month history of changes in behavior and weight loss. The owner reported that the cat had become abnormally unfriendly and would growl or hiss when touched. The cat also had gait changes, manifested by left hind limb weakness, difficulty walking up stairs, and occasionally losing balance and falling down stairs. The cat was examined by its regular veterinarian and had abdominal radiographs, CBC, and biochemistry profile performed, which did not detect any abnormalities. On physical examination, the cat was underweight with an estimated body condition score (BCS) of 1/5. Neurologic examination revealed a very dull mentation, severe generalized muscle atrophy, and a slow, reluctant, and crouched gait. Cranial nerve examination revealed no abnormalities. There was absence of conscious proprioception in all limbs. A forebrain lesion was suspected. The cat was examined 8 days later because of progressive signs of neurologic disease. The cat was obtunded and had a right head turn with a mild right head tilt. The gait showed proprioceptive/right vestibular ataxia with knuckling of both thoracic limbs on ambulation, a crouched posture, and a splaying outward of the left thoracic limb. There was a decreased menace response bilaterally that was worse on the left and decreased nasal sensation bilaterally. Spinal reflexes were normal in all limbs. Neurolocalization was to the right-forebrain with possible brainstem involvement. An abdominal ultrasound was then performed at the owner's request to investigate the gastrointestinal tract as a possible explanation for the weight loss, but no abnormalities were identified.

From the Southern California Veterinary Specialty Hospital, Irvine, CA (Chawla); Department of Veterinary Clinical Sciences, The Ohio State University, Columbus, OH (Cook, Zekas); and Department of Veterinary Biosciences, The Ohio State University, Columbus, OH (Himmel, Oglesbee).

Corresponding author: L. Cook, Department of Veterinary Clinical Sciences, The Ohio State University, 601 Vernon L. Tharp St., Columbus, OH 43210; e-mail: cook.1094@osu.edu.

Submitted May 18, 2015; Revised July 20, 2015; Accepted July 22, 2015.

DOI: 10.1111/jvim.13601

Abbreviations:

CBC	complete blood count
T1 W	T1-weighted MRI
T2 W	T2-weighted MRI
MRI	magnetic resonance imaging
CSF	cerebrospinal fluid
FLAIR	fluid-attenuated inversion recovery

CBC and biochemistry profile showed mild hypercalcemia of 12.4 mg/dL (8–11 mg/dL) and hyperalbuminemia of 4.2 g/dL (2.4–3.9 g/dL). FeLV and FIV ELISA were negative. Brain MRI was performed with a 3 Tesla magnet[a] with the head placed in a knee coil (Philips SENSE Knee-8coil, Acheiva, 8 channel, receive only). After a localizer spin echo sequence, 2 millimeter, contiguous images were acquired using the following sequences: T2-(W)eighted (sagittal, dorsal, and transverse planes), T1-W pre- and postcontrast (sagittal, dorsal and transverse planes), FLAIR transverse, and Fast Field Echo (FFE) transverse. Contrast medium (0.5 mL gadolinium) was administered IV. A 1.9 × 1.9 × 2.9 cm oval to lobular extra-axial mass was identified within the dorsal cerebral cortex on midline with lateral and ventral displacement of the cerebrum. On T1-W images, the mass was iso- to hypointense to the brain parenchyma with a thick anintense rim and amorphous to focal anintense regions internally. Except for the anintense regions, the mass was homogenously, moderately, contrast enhancing. Subjectively, the adjacent dorsal calvarium was mildly thickened (Fig 1a–d). On T2-W and FLAIR sequences, the mass was diffusely hypointense to the brain parenchyma with similar anintense rim and internal foci (Fig 1e–g). On FFE images, the mass was more diffusely anintense with patchy regions which were isointense to brain parenchyma (Fig 1h). There was a focal dilatation of the ventricular system in the region of the quadrigeminal cistern that could have represented a quadrigeminal cyst. The mass effect also caused flattening of the caudal cerebellar margin and protrusion of the cerebellar vermis into the foramen magnum (herniation). Radiographic diagnosis was a mineralized extra-axial mass. Differential diagnoses included meningioma or primary bone neoplasia of the falx cerebri. Intra-axial cerebral neoplasia, granuloma, and chronic hematoma were considered less likely. Cerebellar herniation was secondary to the mass effect.

Surgical debulking was offered, but medical management was elected initially, and the cat was prescribed prednisolone 1.5 mg per os (PO) twice daily.

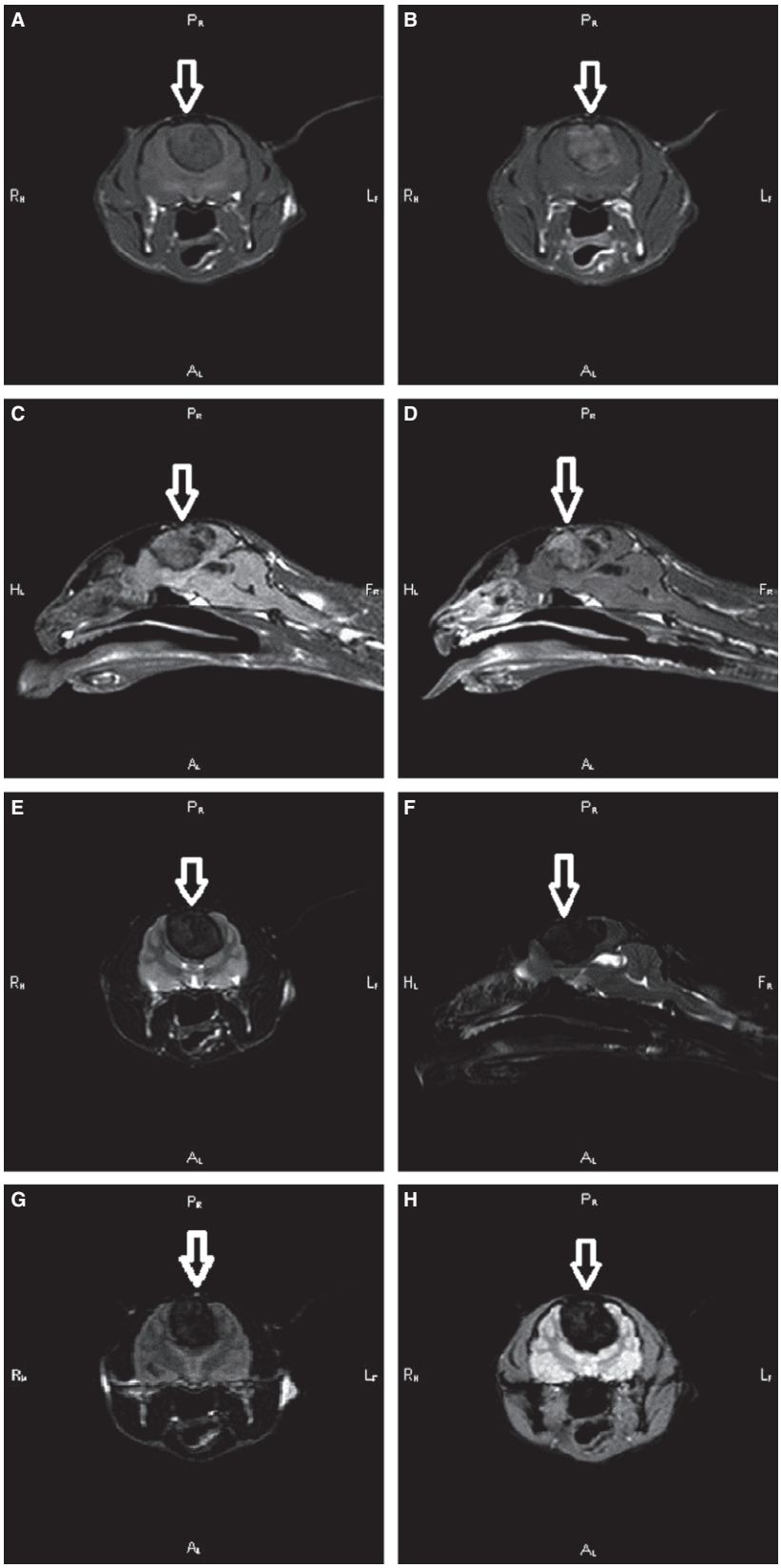

Fig 1. (**a**) T1 W Axial MRI precontrast; (**b**) T1 W Axial MRI postcontrast; (**c**) T1 W Sagittal MRI precontrast; (**d**) T1 W Sagittal MRI postcontrast. The mass is iso- to hypointense to the brain with a thick anintense rim. There is heterogenous contrast enhancement. (**e**) T2 W Axial MRI; (**f**) T2 W Sagittal MRI; (**g**) T2 FLAIR Axial MRI. The mass was heterogenously hypo- to anintense on T2 and FLAIR sequences. (**h**) FFE axial MRI. The mass is diffusely hypointense on FFE. FFE, Fast Field Echo.

The cat was re-presented 7 days after failing to improve on prednisolone treatment to undergo surgery. A right lateral rostrotentorial craniectomy and durotomy were performed. The mass was easily identified and appeared tan to yellow in color and very firm on palpation. The mass was largely debulked. Because of the size of the mass and how far it extended across midline, complete surgical removal could not be achieved. A postoperative CT scan with IV contrast (iohexol 240 mg/mL: 5 mL IV) showed marked reduction in the size of the mass and indistinct margins of contrast enhancement thought to represent residual mass, hemorrhage, or both.

The cat was recovered in ICU and was able to be extubated. She was mentally stuporous and recumbent but would respond to noxious stimuli and would look around and vocalize when handled. She was managed with intravenous isotonic polyionic fluids[b] at 4 mL/kg/h, fentanyl constant rate infusion at 3 μg/kg/h, cefazolin 20 mg/kg IV q12 h, and prednisolone 0.5 mg/kg PO q12 h. She was able to eat small amounts of food. Blood pressure measurement 6 hours postoperatively was 122/86 mmHg. The following morning, approximately 14 hours postoperatively, her mentation appeared to be declining, as she was less responsive. Supportive care with IV fluids, hypertonic saline, and mannitol were administered, but the cat's condition continued to deteriorate, and owner elected euthanasia.

The next day, approximately 24 hours after death, a necropsy was performed. Gross lesions were confined to the brain. Situated within the falx cerebri at the level of the frontal cortices and extending caudally to the level of the corpus callosum, there was a focal, irregularly multinodular, well-demarcated, unencapsulated meningeal mass measuring approximately 5 × 10 × 15 mm (Fig 2a). The mass was tan-brown to yellow, firm, and

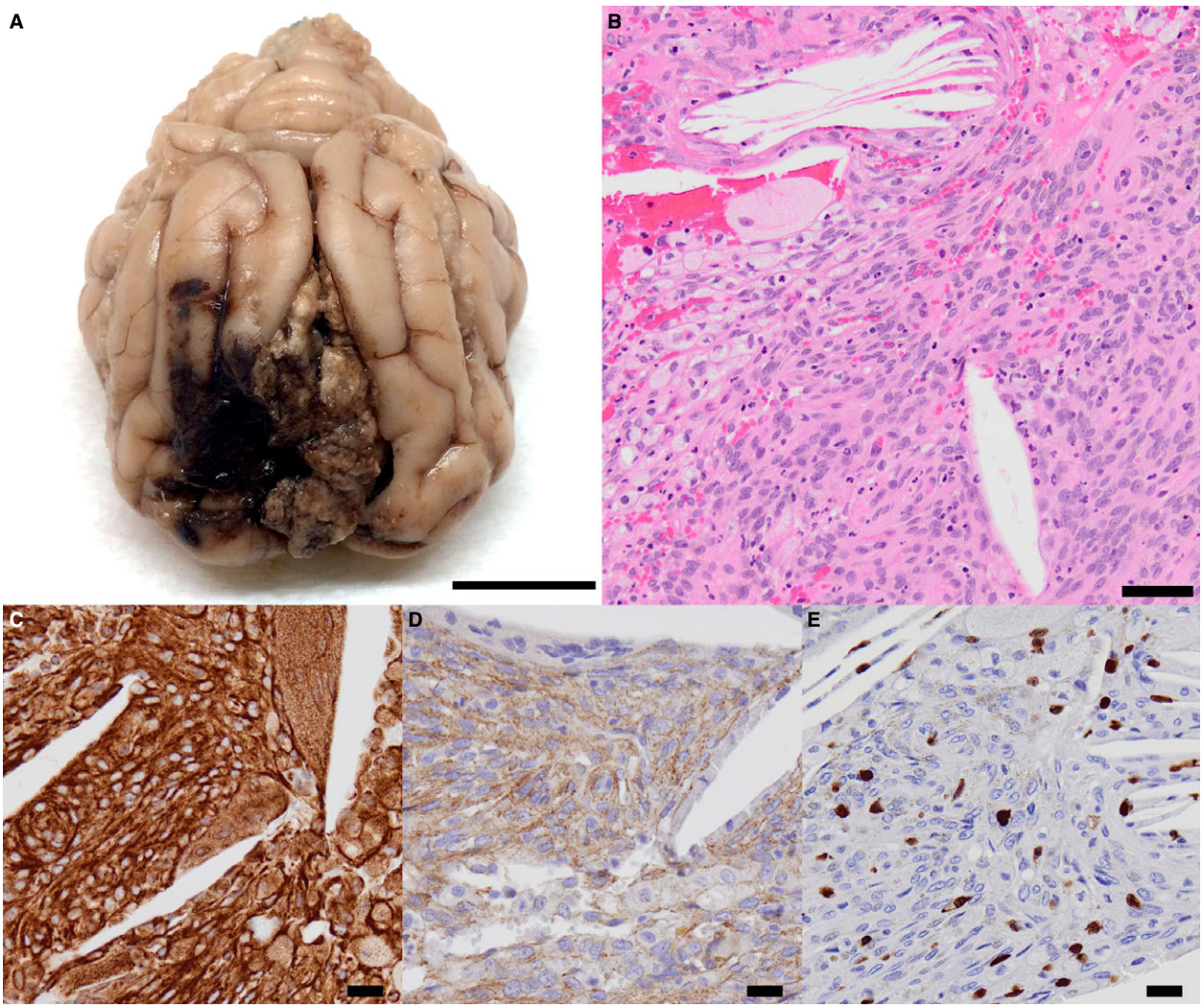

Fig 2. (**a**) Rostrocaudal view of the forebrain mass at postmortem examination. The tumor is tan-brown to yellow and irregularly multinodular with an adjacent focus of hemorrhage at the surgical site. Scale = 1 cm. (**b**) Histopathology of the mass demonstrates a mixture of spindle cells and foamy macrophages with large cholesterol clefts. H&E. Scale = 50 μm. (**c**) Vimentin immunohistochemistry is positive throughout the neoplasm. Scale = 20 μm. (**d**) E-cadherin immunohistochemistry is positive in the spindle cell component of the tumor. Scale = 20 μm. (**e**) Mac387 immunohistochemistry positively labels macrophages within the forebrain mass. Scale = 20 μm.

granular. Adjacent to the meningeal mass, at the site of surgical debulking, there was an approximately 1.5 cm diameter, round defect in the parenchyma of the right frontal cortex which was filled with hemorrhage and fibrin. The caudal portion of the cerebellar vermis protruded slightly through the foramen magnum; no evidence of vascular disturbance was observed, suggesting acute cerebellar herniation. On histopathology, the forebrain mass was found to be originating from the leptomeninges and demonstrating an exophytic, expansile growth pattern, without evidence of invasion into the cerebral cortex. The composition of this mass was uniformly heterogeneous, consisting of one population of spindle-shaped cells arranged in streams and bundles within a sparse, collagenous matrix and a second population of cells characterized as large, foamy macrophages admixed with multinucleated giant cells and neutrophils (Fig 2b). These 2 populations were observed in approximately equal numbers, although the relative proportion varied somewhat throughout the tumor. There were myriad large, oblong to acicular, sharply demarcated, nonstaining cholesterol clefts interspersed throughout the mass. Scattered foci of hemorrhage, hemosiderophages, and mineralization were also found within the tumor. The spindle cell component consisted of mildly pleomorphic cells with indistinct cell borders, a moderate amount of wispy, eosinophilic cytoplasm, and a round to ovoid nucleus containing finely stippled chromatin and 1–2 basophilic nucleoli. Among this population, anisocytosis and anisokaryosis were mild, and occasional mitotic figures were identified. Immunohistochemistry revealed diffuse negative staining for cytokeratin, neuron-specific enolase, and glial fibrillary acidic protein and diffuse positive staining for vimentin (Fig 2c). Two immunohistochemical stains revealed differential staining between the spindle cell population and the inflammatory infiltrate. Neoplastic spindle cells demonstrated finely granular positive cytoplasmic staining for E-cadherin (Fig 2d). Within the same section of brain, histologically normal leptomeninges and choroid plexus also showed positive staining for E-cadherin as an internal positive control (data not shown), whereas sections of lung containing microscopic, subpleural foci of lipogranulomatous inflammation revealed positive E-cadherin staining only in pneumocytes (Fig S1). We interpret positive intratumoral E-cadherin staining as an indicator of meningothelial origin, differentiating these spindle cells from reactive fibroblasts and epithelioid macrophages. Scattered throughout the mass, numerous medium-sized, individual round cells demonstrated strong cytoplasmic staining for Mac387, indicative of macrophage lineage (Fig 2e). Taken together, our findings suggest that this tumor represents a meningothelial neoplasm with concurrent lipogranulomatous inflammation and cholesterol clefts, morphologically diagnosed as both transitional meningioma and cholesterol granuloma.

This case was unusual in that the histopathology was supportive of a cholesterol granuloma formation within a meningioma. Meningiomas are the most common primary brain tumor in cats. They are extra-axial tumors that arise from the arachnoid layer of the leptomeninges. They are variable in size and shape, and there are many histopathologic subtypes. Meningiomas are often firm, encapsulated, discrete masses which can contain mineralization or cystic regions. Hyperostosis of the calvarium adjacent to a meningioma can occur, especially in cats.[1–3] Cats can also develop multiple meningiomas.[3–6] Meningiomas have also been sporadically reported to occur with other neural disorders including meningioangiomatosis[7] and mucopolysaccharidosis type 1.[8] Other differential diagnoses for extra-axial masses in cats include lymphosarcoma, osteosarcoma, and nonneoplastic masses such as granulomas.[3,9] Rarely, solitary cholesterol granuloma formation occurs in the brain of cats.[10–12] Cholesterol cleft formation occurs as a pathologic change within some meningiomas.[13] However, the extensiveness of cholesterol granuloma formation in this cat was considered noteworthy.

Cholesterol granulomas usually occur as primary nonneoplastic masses often involving the choroid plexus and ventricular system,[14,15] but also the falx cerebri[10,11] and petrous apex.[16] They have been most commonly recognized in horses occurring inside or outside of the ventricular system.[14,15,17,18] They occur rarely in humans,[16,19] dogs,[20–22] and other species including meerkats.[23,24] Cholesterol granulomas might cause neurologic signs, but often are incidental findings.

The exact cause of cholesterol granuloma formation is unknown. A lipid metabolism dysfunction has been hypothesized by some.[10] Another hypothesis is chronic deposition of cholesterol crystals as a result of localized chronic inflammation or hemorrhage, cysts, and neoplasms. Erythrocyte and other cellular membrane breakdown could result in accumulation of cholesterol crystals that elicit a foreign body granulomatous reaction.[11–14] Cholesterol crystals might develop as a degenerative/senile change within the choroid plexus presumably from prior hemorrhage.[25]

There is 1 recent case report of a cholesterol granuloma that was adjacent to a meningioma in the brain of a cat.[26] This cholesterol granuloma appeared to develop separately from the meningioma. The mass arose within the lateral and third ventricles, and there was evidence of hemorrhage which could support chronic hemorrhage as a source of the cholesterol granuloma formation in their case. In our case, the mass arose from the falx cerebri within the longitudinal fissure and compressed the lateral and third ventricles.[26] This cholesterol granuloma appeared to develop within the meningioma. There was some histopathologic evidence of hemorrhage which could be one cause of the cholesterol granuloma formation. Other possible causes include inflammation resulting from the meningioma such as coagulation necrosis that may be present with a large tumor, meningeal cell breakdown resulting in cholesterol crystal deposition, or a combination of these factors.

Magnetic resonance imaging features of the mass in our case demonstrated similarities with the previously published cholesterol granulomas reported in cats. All cases showed areas of hypo/anintensity on T2-weighted

images as well as a hypointense peripheral rim around the mass in all sequences.[10,11,26] Inner regions of the mass were nonhomogenous with primarily hypointense regions on T2, T1, and FLAIR images with nonhomogenous but fairly robust contrast enhancement.[10,11,26] Subjectively, there was more contrast enhancement in our case and in the previously published meningioma-cholesterol granuloma case than in the other 2 cases of primary cholesterol granuloma in cats. This could be explained by the presence of the meningioma, which are known to contrast enhance strongly both in dogs and cats[1,2,5,10,11,26] suggesting that more contrast enhancement on MR images would favor a diagnosis of meningioma or meningioma-cholesterol granuloma over a solitary cholesterol granuloma.

This case was a unique presentation of an unusually large cholesterol granuloma that appeared to develop within a meningioma. Cholesterol granuloma or cholesterol granuloma-meningioma should be considered as a differential in cats with large ventricular system or falcine mass lesions.

Footnotes

[a] Philips Achieva 3T, Cleveland, OH.
[b] Plasma-Lyte A®; Abbot Laboratories, North Chicago, IL.

Acknowledgments

Conflict of Interest Declaration: Authors disclose no conflict of interest.

Off-label Antimicrobial Declaration: Authors declare no off-label use of antimicrobials.

References

1. Motta L, Mandara MT, Skerritt GC. Canine and feline intracranial meningiomas: An updated review. Vet J 2012;192:153–165.

2. Sessums K, Mariani C. Intracranial meningioma in dogs and cats: A comparative review. Compend Contin Educ Vet, 2009;31:330–339.

3. Tomek A, Cizinauskas S, Doherr M, et al. Intracranial neoplasia in 61 cats: Localisation, tumour types and seizure patterns. J Feline Med Surg 2006;8:243–253.

4. Troxel MT, Van Winkle TJ, Newton AL, et al. Feline intracranial neoplasia: Retrospective review of 160 cases (1985–2001). J Vet Intern Med 2003;17:850–859.

5. Forterre F, Tomek A, Konar M, et al. Multiple meningiomas: Clinical, radiological, surgical, and pathological findings with outcome in four cats. J Feline Med Surg 2007;9:36–43.

6. Lu D, Pocknell A, Lamb CR, et al. Concurrent benign and malignant multiple meningiomas in a cat: Clinical, MRI and pathological findings. Vet Rec 2003;152:780–782.

7. Ginel PJ, Novales M, Blanco B, et al. Meningioangiomatosis associated with fibrous meningioma in a dog. Vet Rec 2009; 164:756–758.

8. Haskins ME, McGrath JT. Meningiomas in young cats with mucopolysaccharidosis I. J Neuropathol Exp Neurol 1983;42:664–670.

9. Troxel MT, Massicotte C, McLear RC, et al. Magnetic resonance imaging features of feline intracranial neoplasia: Retrospective analysis of 46 cats. J Vet Intern Med 2004;18:176–189.

10. Fluehmann G, Konar M, Jaggy A, et al. Cerebral cholesterol granuloma in a cat. J Vet Intern Med 2006;20:1241–1244.

11. Ricci E, Abbiati G, Cantile C. Intracranial cholesterol granuloma in a cat. J Vet Med Sci 2010;72:1475–1478.

12. Faller K, Leach J, Gutierrez-Quintana R, et al. Diagnostic exercise: Circling and behavioral changes in a cat. Vet Pathol, 2014;52:696–699.

13. Wills TB, Chen AV, Haldorson GJ. What is your diagnosis? Intracranial mass in a cat. Vet Clin Pathol 2009;38:39–41.

14. Jackson CA, de Lahunta A, Dykes NL, et al. Neurological manifestation of cholesterinic granulomas in three horses. Vet Rec 1994;135:228–230.

15. Vink-Nooteboom M, Junker K, van den Ingh TS, et al. Computed tomography of cholesterinic granulomas in the choroid plexus of horses. Vet Radiol Ultrasound 1998;39:512–516.

16. Gore MR, Zanation AM, Ebert CS, et al. Cholesterol granuloma of the petrous apex. Otolaryngol Clin North Am 2011;44:1043–1058.

17. Duff S. Cholesterinic granulomas in horses. Vet Rec 1994;135:288.

18. Johnson PJ, Lin TL, Jennings DP. Diffuse cerebral encephalopathy associated with hydrocephalus and cholesterinic granulomas in a horse. J Am Vet Med Assoc 1993;203:694–697.

19. Grossi PM, Ellis MJ, Cummings TJ, et al. Cholesterol granuloma of the lateral ventricle. Case report. J Neurosurg 2008;108:357–360.

20. Cramer SD, Miller AD, Medici EL, et al. Sellar xanthogranuloma in a dog. J Vet Diagn Invest 2011;23:387–390.

21. Lovett MC, Fenner WR, Watson AT, et al. Imaging diagnosis-MRI characteristics of a fourth ventricular cholesterol granuloma in a dog. Vet Radiol Ultrasound 2012;53:650–654.

22. Steiss JE, Cox NR, Knecht CD. Electroencephalographic and histopathologic correlations in eight dogs with intracranial mass lesions. Am J Vet Res 1990;51:1286–1291.

23. Allan KJ, Waters M, Ashton DG, et al. Meningeal cholesterol granulomas in two meerkats (*Suricata suricatta*). Vet Rec 2006;158:636–637.

24. Sladky KK, Dalldorf FG, Steinberg H, et al. Cholesterol granulomas in three meerkats (*Suricata suricatta*). Vet Pathol 2000;37:684–686.

25. Maxie MG. Nervous system. In: Maxie M, ed. Pathology of Domestic Animals, 5th ed., Vol. 3. Philadelphia, PA: Elsevier Saunders Ltd; 2007:335–343.

26. Ondreka N, Henrich M, Kramer M, et al. Co-occurrence of an intraventricular meningioma and cholesterol granuloma of the choroid plexus in a cat. Tierarztl Prax Ausg K Kleintiere Heimtiere, 2013;41:408–412.

Supporting Information

Additional Supporting Information may be found online in Supporting Information:

Fig S1. E-cadherin immunohistochemistry in foci of subpleural lipogranulomatous inflammation shows positive staining only in pneumocytes. Scale = 50 μm.